JACS
JOURNAL OF THE AMERICAN CHEMICAL SOCIETY

Communication

pubs.acs.org/JACS

The Fixed Propeller-Like Conformation of Tetraphenylethylene that Reveals Aggregation-Induced Emission Effect, Chiral Recognition, and Enhanced Chiroptical Property

Jia-Bin Xiong,[†] Hai-Tao Feng,[†] Jian-Ping Sun,[†] Wen-Zhao Xie,[†] Dong Yang,[‡] Minghua Liu,[‡] and Yan-Song Zheng*[,†]

[†]Key Laboratory of Material Chemistry for Energy Conversion and Storage, Ministry of Education, School of Chemistry and Chemical Engineering, Huazhong University of Science and Technology, Wuhan 430074, China

[‡]Beijing National Laboratory for Molecular Science (BNLMS), CAS Key Laboratory of Colloid Interface and Chemical Thermodynamics, Institute of Chemistry, Chinese Academy of Sciences, Beijing 100190, China

Supporting Information

ABSTRACT: The propeller-like conformation of tetraphenylethylene (TPE) with aggregation-induced emission (AIE) effect was partially and completely fixed by intramolecular cyclization for the first time. The immobilization of propeller-like conformation was found to show great advantages in determining the enantiomer purity, identifying the chiral amines. The completely fixed conformers are resolved into *M*- and *P*-enantiomer, which showed mirror imaged CD and almost quantitative fluorescence quantum yield. Furthermore, it also showed a mirror and large circularly polarized luminescence dissymmetric factor, depending on the helicity of the enantiomer. The result provides the most direct and persuasive evidence for AIE via the restriction of intramolecular rotation and finds the new insight of the compounds in chiroptical property.

Aggregation-induced emission (AIE) phenomenon arouses wide attention due to enormous application potential in chemo/biosensors and optoelectronic materials.[1−3] For most of compounds with AIE effect, such as tetraphenylethylene (TPE), hexaphenylsilole (HPS), and their derivatives, they all bear a propeller-like conformation which is the key structural feature why they display AIE phenomenon. By immobilization of propeller-like conformation of AIE compounds, on one hand, it will provide novel propeller-like molecules with helical chirality and high fluorescence quantum yield, which have exhibited many possible utilizations in adjustment of physiological functionalities, chiral sensor, asymmetric catalyst, and displaying materials et al.[4−11] On the other hand, it also affords the most direct and persuasive evidence for popular AIE mechanism of restriction of intramolecular rotation (RIR) that is still in dispute[2] because it will display fluorescence precisely according to the RIR process. However, no literature about immobilization of propeller-like conformation of AIE molecules is documented to date.

In order to enhance fluorescence intensity and corroborate the RIR principle, efforts to restrict the rotation of phenyl rings by covalent bond connection have been made. It is reported that phenyl rotation of TPE unit is blocked by covalent single bond between phenyl rings, but the propeller-like structure is lost.[12−14] By using ethylene or vinylene tethers to connect two gem-phenyl rings at the ortho position, restriction of phenyl rotation is also achieved, but the obtained TPE derivatives are nonhelical.[15] Forming molecular cage,[16] metallacage,[17] metal organic frameworks,[18−20] or covalent organic frameworks[21,22] based on TPE cores, the phenyl rotation is blocked that leads to strong fluorescence, but no helical chirality from the propeller-like conformation of TPE units is obtained and exploited. Here, we report that TPE molecule, which is the most typical and the most studied AIE compound, is bridged between its four phenyl rings by short tethers to give TPE tetracycle with stable propeller-like structure in solution, which is resolved into *M*- and *P*-enantiomers.

Immobilization route of TPE propeller-like conformation is shown in Figure 1. In the ^{1}H NMR spectrum, methylene protons of TPE dicycle tetraldehyde **3** appeared with two double peaks, while a similar TPE monocycle displayed a single peak for methylene groups in literature.[23] This indicated that the rotation of the phenyl rings of TPE unit of **3** was no longer completely free, resulting in a difference of two protons in the methylene groups. For tetrahydroxymethyl TPE dicycle **4**, the methylene groups on cycle also showed two double peaks, while two protons of the hydroxymethyl groups were in the same chemical environment because of free rotation. In the ^{1}H NMR spectrum of TPE tetracycle **6**, two sets of methylene groups all exhibited double peaks, demonstrating the blockage of the phenyl rotation put the two protons of any methylene group into a different chemical environment.

As expected from RIR mechanism, TPE dicycle **3**, **4** and TPE tetracycle **6** not only showed strong blue fluorescence in suspension in 95:5 H_2O/THF (volume ratio, the same below) or in solid state but also emitted intensive light in solution (Figure 2A,B). Moreover, **6** bearing four cycles could emit green fluorescence even under daylight (Figure 2C). The relative fluorescence quantum yield of **2**−**4** and **6**, measured using fluorescein as standard, increased with the number of cycles. From **2**−**4** to **6**, the fluorescence quantum yields in THF solution were 0%, 24%, 49%, and 97%, and those in 95:5 H_2O/THF suspension were 2%, 22%, 51%, and 80%, respectively.

Received: July 9, 2016
Published: August 26, 2016

DOI: 10.1021/jacs.6b07087
J. Am. Chem. Soc. 2016, 138, 11469−11472

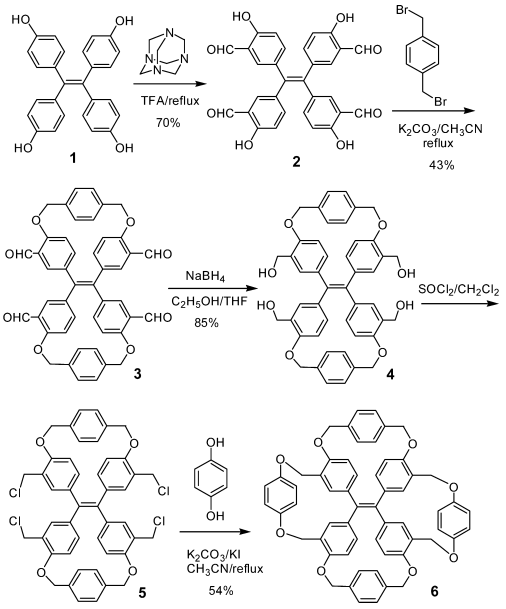

Figure 1. Synthetic route of TPE helical molecules **3**–**6** with stable and metastable propeller-like conformations.

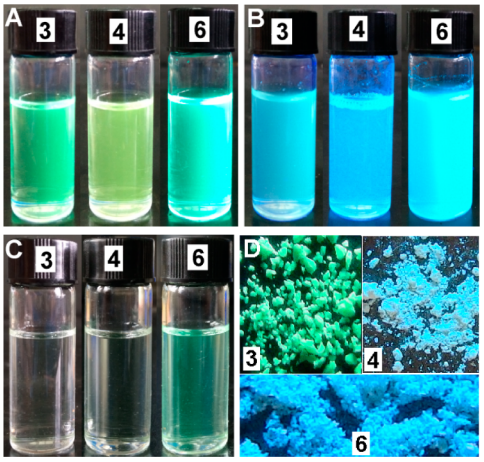

Figure 2. Photos of **3**, **4**, and **6** in THF solution under 365 nm UV light (A), in 95:5 H_2O/THF suspension under 365 nm UV light (B), in THF solution under daylight (C), and as dry powder under 365 nm UV light (D). [**3**] = [**4**] = [**6**] = 1.0×10^{-4} M.

Moreover, the fluorescence intensity of **3**, **4**, and **6** in THF always increased with increasing concentration (Figures S28–S30).

In addition, while **3**, **4**, and **6** had emission maximum wavelengths at 508, 527, and 492 nm in THF solution, they emit at 475, 459, and 484 nm upon aggregation in 95:5 H_2O/THF, showing hypsochromic shifts of 33, 68 and 8 nm, respectively (Figures S31–S33). As crystals freshly isolated from THF solution, **3**, **4**, and **6** also exhibited hypsochromic shifts of 37, 50, and 31 nm, respectively, compared with THF solution. When the crystals were dried and became powder, the emission hypsochromic shifts of **3**, **4**, and **6** were 17, 59, and 11 nm, respectively, compared with the THF solution (Figure 2D).

Crystal structure of **3** disclosed that the cycles spanned onto two phenyl groups at the *cis*-position rather than two phenyl rings at the *gem*-position (Figure S34).[24] In one unit cell, both left-handed helical (*M*) TPE cores and right-handed helical (*P*) ones were equally observed. Although racemic **3** could be resolved into *M*-**3** and *P*-**3** enantiomers using chiral high-pressure liquid chromatography (HPLC), the obtained enantiomers rapidly racemized in solution at room temperature, indicating that *M*-**3** and *P*-**3** enantiomers could interconvert due to not fully inhibiting the phenyl rotation.

Interestingly, this metastable propeller-like structure could be exploited to determine the enantiomeric composition of chiral amines when racemic **3** was biased into a single helical propeller-like one in the reaction of amine enantiomer and **3**.[25−30] In the presence of acetic acid, **3** could immediately react with a chiral primary amine such as **7**–**13** and reach dynamic equilibrium in about 0.5 h (Figure S35). Moreover, **3** could induce obvious CD signals by amine enantiomers which had no or very weak CD signals (Figures 3 and S36–S37). For example, while *R*- or *S*-**7**

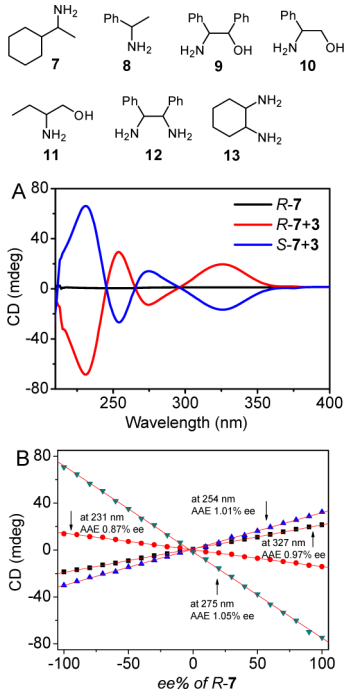

Figure 3. Structure of chiral amines. (A) CD spectra of the solution of enantiomer of **7** and acetic acid (HAc) with and without **3** in 1,2-dichloroethane. (B) Change in CD intensity with ee% of *R*-**7**, the red line is the linear fitting result. [**3**] = 1/10[**7**] = 1/20[HAc] = 2.0×10^{-4} M.

was CD silent, the mixture of enantiomers and **3** displayed strong CD signals with a perfect mirror image each other (Figure 3A). Under the same conditions, the mixture of amine enantiomers and **2** showed no or a much weaker CD band, except for **11** which probably led to a different dynamical equilibrium (Figure S38), hinting that **3** more easily produced a dynamically stable single helical propeller-like structure due to partial rotation fixation.

With an increase of *R*-**7** concentration, the CD profile did not change, but the intensity increased. Above 10:1 molar ratio of *R*-**7** to **3**, the CD intensity was saturated (Figure S39). Interestingly, the fluorescence intensity also increased with a molar ratio larger than 4. Moreover, at <8, the emission displayed a gradual bathochromic shift from 505 to 526 nm with the molar ratio (Figure S40). After a molar ratio of 8, no bathochromic shift was observed, and meanwhile the CD intensity leveled off, indicating dynamical equilibrium of the condensation reaction.

Such induced CD can be further used to determine the enantiomer excess (ee) values of the chiral amines. Keeping the molar ratio of **7** to **3** at 10:1, the ee% of *R*-**7** in the mixture of *R*-**7**

DOI: 10.1021/jacs.6b07087
J. Am. Chem. Soc. 2016, 138, 11469−11472

and *S*-**7** increased linearly with the CD intensity, as shown in Figures 3B and S41. These straight lines were used as a calibration curve for determining enantiomer content of eight samples with unknown ee%. The average absolute error (AAE) between measured ee values and actual ones was 0.97% ee at 327 nm, 1.05% ee at 275 nm, 1.01% ee at 254 nm, and 0.87% at 231, which are much smaller than reported in literature.[27−30] Other chiral amines, such as **9** and **12**, also exhibited a perfect linear relationship between CD intensity and ee% with an AAE <1.50% (Figure S42−S43). In addition, CD signals of **3** with all amines exhibited multiple characteristic bands with different shape and intensity,[29,30] which could be utilized to identify these chiral amines.

The crystal structure of **6** confirmed that it bore four cycles and had slipped packing of the propeller-like structures that did not form intermolecular $\pi-\pi$ stacking (Figure S44).[24] Just like **3**, *M*-**6** and *P*-**6** equally existed in one unit cell, and molecules with the same helical chirality packed into column structures (Figure S44B). Noticeably, the twisted angle of the TPE core double bond was up to 20.90°, while it was 12.6° in the structure of **3**, implying that the twisted structure of TPE derivatives did not lead to emission quenching.

As expected, **6** could be resolved into two stable single helical enantiomers by chiral HPLC using a CHIRALPAK IE column and 80:20 CH_2Cl_2/CH_3OH mobile phase. Crystal structure of one enantiomer related to the first peak in HPLC unveiled only one single left-handed helical structure in the unit cell, which was *M*-**6** (Figure 4A). Other enantiomer related to the second peak

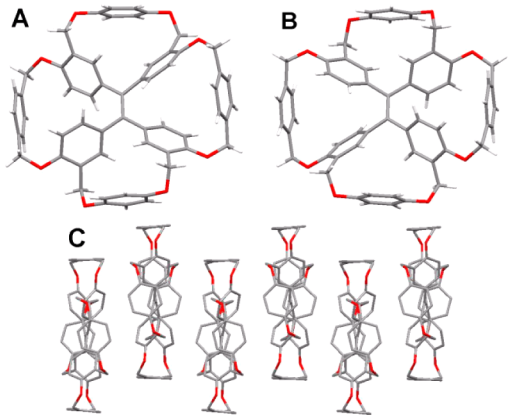

Figure 4. Crystal structure of *M*-**6** (A), *P*-**6** (B), and packing of *M*-**6** (C). The protons in C and the solvents in A−C were removed for clarity.

was right-handed helical in the crystal structure and was *P*-**6** (Figure 4B).[24] Similar to racemic **6**, the molecules of *M*-**6** and *P*-**6** packed into the column structure. Although the packing of the enantiomer was slipped much less than that of racemic **6** (Figure 4C), $\pi-\pi$ stacking was also absent. *M*-**6** had a specific optical rotation of +479°, while that of *P*-**6** was −502° in THF. With identical ^{1}H NMR, ^{13}C NMR, and HRMS spectra, these two resolved compounds were corroborated to be enantiomers of each other. In CD spectrum, *M*-**6** showed a strong positive first Cotton effect and positive bisignate band, while *P*-**6** showed negative ones with a similar intensity (Figure 5A), showing a perfect mirror image relationship.

Just like racemic **6**, *M*-**6** and *P*-**6** emitted strong fluorescence both in solution and in aggregation state and showed identical absorption and emission spectra (Figures S25−S27). The relative fluorescence quantum yield was 100% and 100% in

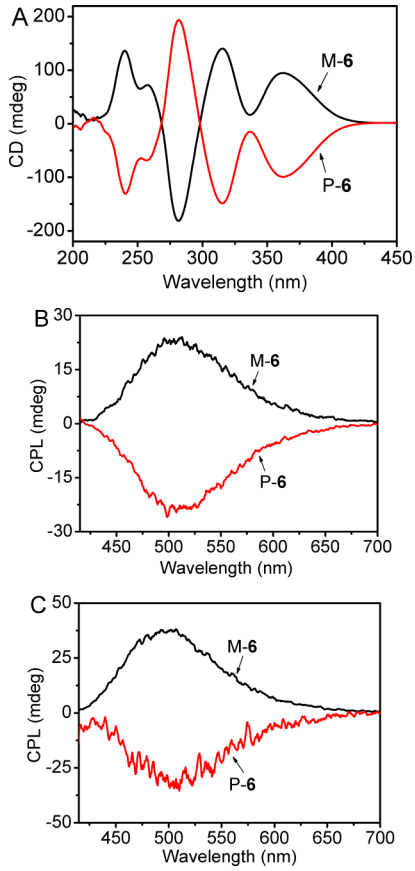

Figure 5. CD spectra (A) and CPL spectra (B) of *M*-**6** and *P*-**6** in THF (1.0×10^{-3} M); CPL spectra (C) of *M*-**6** and *P*-**6** in 90:10 H_2O/THF (1.0×10^{-3} M). Excited at 365 nm.

solution and 82% and 81% in 90:10 H_2O/THF suspension for *M*-**6** and *P*-**6**, respectively, measured using fluorescein as standard. Furthermore, the absolute fluorescence quantum yield, measured by integrate sphere, was found to be 79%, 94%, and 94% in solution and 88%, 85%, and 86% in the suspension for **6**, *M*-**6**, and *P*-**6**, respectively, which was in line with the relative fluorescence quantum yield.

Meanwhile, similar to racemic **6**, *M*-**6** and *P*-**6** emitted green light in solution even under daylight, but blue fluorescence was observed in the aggregation or crystal state with a hypsochromic shift of about 10 nm. It is well-known that emission maximum wavelength of AIE compounds, especially that of TPE derivatives, is very sensitive to external factors such as solvent, pressure, aggregation states, and so on.[2] These factors affect rotation degrees of phenyl rings that either increase or attenuate conjugation of the AIE molecules so that a chromic response appears. Although the phenyl rings of TPE core of **6** were immobilized and could not rotate freely, they were not fixed very tightly, and the swing or flipping[19] of the phenyl rings in a range of several degrees still existed, which could change the conjugation of TPE unit among small angles. The mechanochromic effect of **3**, **4**, and **6** under grinding also demonstrated the above description (Figure S45). This suggested that RIR was the main reason for fluorescence occurrence and enhancement rather than other motions.

Significantly, obvious circularly polarized luminescence (CPL)[31−35] signals of *M*-**6** and *P*-**6** with mirror image at 505 nm in THF solution and 500 nm in 95:5 H_2O/THF suspension were observed (Figure 5B,C). In solution, the CPL dissymmetric

DOI: 10.1021/jacs.6b07087
J. Am. Chem. Soc. 2016, 138, 11469−11472

factor (g_{lum}) was $+3.1 \times 10^{-3}$ for *M*-**6** and -3.3×10^{-3} for *P*-**6**. In suspension, the $|g_{lum}|$ was about 1-fold larger than that in solution, which was $+6.2 \times 10^{-3}$ for *M*-**6** at 495 nm and -5.0×10^{-3} for *P*-**6** at 505 nm. The $|g_{lum}|$ of the enantiomers of **6** was large when related to the $|g_{lum}|$ of $10^{-5}-10^{-2}$ for general organic compounds. In addition, the $|g_{lum}|$ was close to the dissymmetry factor of absorbance ($g_{abs} = 2(\Delta\varepsilon/\varepsilon)$) of 2.4×10^{-3} for *M*-**6** and *P*-**6**, suggesting that the conformational change between ground and excited states was little.[31,32] The mixtures of **3** and enantiomers of **7** were also tested for CPL spectrum, but no CPL signal was observed. These results demonstrated that the single helical propeller-like second-ordered structure of TPE fixed by four bridges was conformationally stable. In fact, when the solution of *M*-**6** and *P*-**6** in THF was left to stand at room temperature for more than one month, no racemization was observed.

In conclusion, the propeller-like conformation of the TPE unit that is the key factor for most of organic compounds showing AIE effects was immobilized for the first time. The immobilization of the propeller-like conformation could afford rapid and accurate measurements of enantiomeric purity, helical chirality from *M*- and *P*-enantiomers, and the most direct and persuasive evidence for a RIR AIE mechanism. While the almost quantitative fluorescence quantum yield of TPE tetracycle **6** made it an excellent candidate in fluorophore dyes, its two enantiomers showing a large CPL dissymmetric factor would have great potential in 3D display and medical imaging besides potential usage in chiral recognition and enantioselective catalysis. The bridging between rotors of AIE compounds by a short spacer provided a new approach to helical chiral compounds with high fluorescence quantum yield.

■ ASSOCIATED CONTENT

Supporting Information

The Supporting Information is available free of charge on the ACS Publications website at DOI: 10.1021/jacs.6b07087.

Experimental details and data (PDF)
Characterization data (CIF)
Characterization data (CIF)
Characterization data (CIF)
Characterization data (CIF)

■ AUTHOR INFORMATION

Corresponding Author

*zyansong@hotmail.com

Notes

The authors declare no competing financial interest.

■ ACKNOWLEDGMENTS

We thank National Natural Science Foundation of China (21072067) and HUST Interdisciplinary Innovation Team (2015ZDTD055) for financial support and the Analytical and Testing Centre at Huazhong University of Science and Technology for measurement.

■ REFERENCES

(1) Luo, J.; Xie, Z.; Lam, J. W. Y.; Cheng, L.; Chen, H.; Qiu, C.; Kwok, H. S.; Zhan, X.; Liu, Y.; Zhu, D.; Tang, B. Z. *Chem. Commun.* **2001**, 1740.
(2) Mei, J.; Leung, N. L. C.; Kwok, R. T. K.; Lam, J. W. Y.; Tang, B. Z. *Chem. Rev.* **2015**, *115*, 11718.
(3) Ding, D.; Li, K.; Liu, B.; Tang, B. Z. *Acc. Chem. Res.* **2013**, *46*, 2441.
(4) Shinohara, K-i.; Sannohe, Y.; Kaieda, S.; Tanaka, K.-i.; Osuga, H.; Tahara, H.; Xu, Y.; Kawase, T.; Bando, T.; Sugiyama, H. *J. Am. Chem. Soc.* **2010**, *132*, 3778.
(5) Zhang, G.-W.; Li, P.-F.; Meng, Z.; Wang, H.-X.; Han, Y.; Chen, C.-F. *Angew. Chem., Int. Ed.* **2016**, *55*, 5304.
(6) Katoono, R.; Kawai, H.; Fujiwara, K.; Suzuki, T. *J. Am. Chem. Soc.* **2009**, *131*, 16896.
(7) Huo, H.; Shen, X.; Wang, C.; Zhang, L.; Röse, P.; Chen, L.-A.; Harms, K.; Marsch, M.; Hilt, G.; Meggers, E. *Nature* **2014**, *515*, 100.
(8) Zhang, L.; Wang, T.; Shen, Z.; Liu, M. *Adv. Mater.* **2016**, *28*, 1044.
(9) Gingras, M. *Chem. Soc. Rev.* **2013**, *42*, 1051.
(10) Yamagishi, H.; Fukino, T.; Hashizume, D.; Mori, T.; Inoue, Y.; Hikima, T.; Takata, M.; Aida, T. *J. Am. Chem. Soc.* **2015**, *137*, 7628.
(11) Martinez, A.; Guy, L.; Dutasta, J.-P. *J. Am. Chem. Soc.* **2010**, *132*, 16733.
(12) Shi, J.; Chang, N.; Li, C.; Mei, J.; Deng, C.; Luo, X.; Liu, Z.; Bo, Z.; Dong, Y. Q.; Tang, B. Z. *Chem. Commun.* **2012**, *48*, 10675.
(13) Tong, H.; Dong, Y.; Hong, Y.; Häussler, M.; Lam, J. W. Y.; Sung, H. H. Y.; Yu, X.; Sun, J.; Williams, I. D.; Kwok, H. S.; Tang, B. *J. Phys. Chem. C* **2007**, *111*, 2287.
(14) Wang, J.-H.; Feng, H.-T.; Luo, J.; Zheng, Y.-S. *J. Org. Chem.* **2014**, *79*, 5746.
(15) Leung, N. L.; Xie, N.; Yuan, W.; Liu, Y.; Wu, Q.; Peng, Q.; Miao, Q.; Lam, J. W. Y.; Tang, B. Z. *Chem. - Eur. J.* **2014**, *20*, 15349.
(16) Zhang, C.; Wang, Z.; Tan, L.; Zhai, T.-L.; Wang, S.; Tan, B.; Zheng, Y.-S.; Yang, X.-L.; Xu, H.-B. *Angew. Chem.* **2015**, *127*, 9376.
(17) Yan, X.; Cook, T. R.; Wang, P.; Huang, F.; Stang, P. J. *Nat. Chem.* **2015**, *7*, 342.
(18) Shustova, N. B.; McCarthy, B. D.; Dincă, M. *J. Am. Chem. Soc.* **2011**, *133*, 20126.
(19) Shustova, N. B.; Ong, T.-C.; Cozzolino, A. F.; Michaelis, V. K.; Griffin, R. G.; Dincă, M. *J. Am. Chem. Soc.* **2012**, *134*, 15061.
(20) Wei, Z.; Gu, Z.-Y.; Arvapally, R. K.; Chen, Y.-P.; McDougald, R. N., Jr; Ivy, J. F.; Yakovenko, A. A.; Feng, D.; Omary, M. A.; Zhou, H.-C. *J. Am. Chem. Soc.* **2014**, *136*, 8269.
(21) Dalapati, S.; Jin, E.; Addicoat, M.; Heine, T.; Jiang, D. *J. Am. Chem. Soc.* **2016**, *138*, 5797.
(22) Zhou, T.-Y.; Xu, S.-Q.; Wen, Q.; Pang, Z.-F.; Zhao, X. *J. Am. Chem. Soc.* **2014**, *136*, 15885.
(23) Feng, H.-T.; Wang, J.-H.; Zheng, Y.-S. *ACS Appl. Mater. Interfaces* **2014**, *6*, 20067.
(24) The crystallographic data of compounds **3**, **6**, *M*-**6**, and *P*-**6** have been deposited in the Cambridge Structural Database as CCDC 1484752, 1484754, 1484753, and 1484755, respectively.
(25) Yashima, E.; Maeda, K.; Okamoto, Y. *Nature* **1999**, *399*, 449.
(26) Yashima, E.; Matsushima, T.; Okamoto, Y. *J. Am. Chem. Soc.* **1997**, *119*, 6345.
(27) You, L.; Zha, D.; Anslyn, E. V. *Chem. Rev.* **2015**, *115*, 7840.
(28) Bentley, K. W.; Nam, Y. G.; Murphy, J. M.; Wolf, C. *J. Am. Chem. Soc.* **2013**, *135*, 18052.
(29) Yang, Y.; Pei, X.-L.; Wang, Q.-M. *J. Am. Chem. Soc.* **2013**, *135*, 16184.
(30) Joyce, L. A.; Sherer, E. C.; Welch, C. J. *Chem. Sci.* **2014**, *5*, 2855.
(31) Morisaki, Y.; Gon, M.; Sasamori, T.; Tokitoh, N.; Chujo, Y. *J. Am. Chem. Soc.* **2014**, *136*, 3350.
(32) Sánchez-Carnerero, E. M.; Moreno, F.; Maroto, B. L.; Agarrabeitia, A. R.; Ortiz, M. J.; Vo, B. G.; Muller, G.; de la Moya, S. *J. Am. Chem. Soc.* **2014**, *136*, 3346.
(33) Tang, Y.; Cohen, A. E. *Science* **2011**, *332*, 333.
(34) Okano, K.; Taguchi, M.; Fujiki, M.; Yamashita, T. *Angew. Chem., Int. Ed.* **2011**, *50*, 12474.
(35) Shen, Z.; Wang, T.; Shi, L.; Tang, Z.; Liu, M. *Chem. Sci.* **2015**, *6*, 4267.

DOI: 10.1021/jacs.6b07087
J. Am. Chem. Soc. 2016, 138, 11469−11472